JOC The Journal of Organic Chemistry

Article

pubs.acs.org/joc

Microwave-Based Reaction Screening: Tandem Retro-Diels–Alder/Diels–Alder Cycloadditions of *o*-Quinol Dimers

Suwei Dong,[†] Katharine J. Cahill,[‡] Moon-Il Kang,[§] Nancy H. Colburn,[§] Curtis J. Henrich,[§] Jennifer A. Wilson,[§] John A. Beutler,[§] Richard P. Johnson,*[,‡] and John A. Porco, Jr.*[,†]

[†]Department of Chemistry and Center for Chemical Methodology and Library Development (CMLD-BU), Boston University, Boston, Massachusetts 02215, United States

[‡]Department of Chemistry, University of New Hampshire, Durham, New Hampshire 03824, United States

[§]Laboratory of Cancer Prevention and Molecular Targets Laboratory, Center for Cancer Research, NCI-Frederick, Frederick, Maryland 21702, United States

Supporting Information

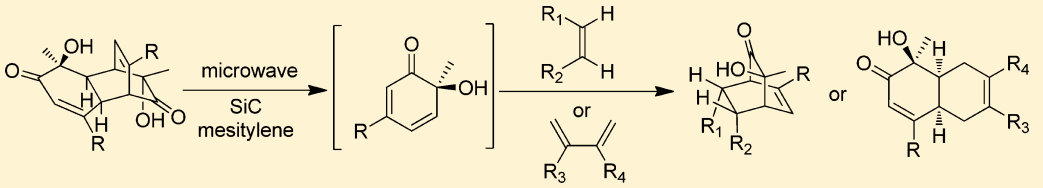

ABSTRACT: We have accomplished a parallel screen of cycloaddition partners for *o*-quinols utilizing a plate-based microwave system. Microwave irradiation improves the efficiency of retro-Diels–Alder/Diels–Alder cascades of *o*-quinol dimers which generally proceed in a diastereoselective fashion. Computational studies indicate that asynchronous transition states are favored in Diels–Alder cycloadditions of *o*-quinols. Subsequent biological evaluation of a collection of cycloadducts has identified an inhibitor of activator protein-1 (AP-1), an oncogenic transcription factor.

INTRODUCTION

o-Quinols are highly reactive 2,4-cyclohexadienones and have been proposed as precursors for a number of natural products. *o*-Quinol dimers are common building blocks for preparation of bicyclo[2.2.2]octenones via retro-Diels–Alder reaction followed by a Diels–Alder cycloaddition with external dienophiles.[1] We recently reported the synthesis of the natural product chamaecypanone C (**1**)[2] involving a retro-Diels–Alder/Diels–Alder cascade of 2,4-cyclohexadienone (*o*-quinol) dimer **2** and diaryl enone **3** under thermal, oxidative conditions (Scheme 1). [4 + 2] cycloaddition of the derived *o*-quinol monomer **4** and 2,4-diaryl cyclopentadienone **5** was found to proceed in a highly regio- and diastereoselective manner. This result, along with reactions with a few dienophiles, prompted us to further evaluate cycloadditions of **4** and related *o*-quinols with a range of reaction partners, in order to better understand the mode of reactivity for dienophiles as well as diastereoselectivity with respect to the *o*-quinol.

Retro-[4 + 2]/[4 + 2] reactions of dimers derived from *o*-quinols and masked *o*-benzoquinones (MOBs) have been utilized for the preparation of reactive 2,4-cyclohexadienones en route to bicyclo[2.2.2]octenones.[1,3,4] However, most reported examples involve thermolysis at high temperatures for extended reaction times. In some cases, sealed tubes have been used at temperatures up to 220 °C,[3b] where safety issues may become a concern. In comparison to conventional heating, microwave heating has been proven to be efficient in many cases, leading to a dramatic reduction in reaction time.[5] In particular, use of thermal susceptors or "sensitizers", including graphite[6] and silicon carbide (SiC),[7] has been shown to further improve the efficiency of thermal transformations, as these materials can reach high temperature under microwave irradiation in spite of the nature of reaction solvents.[8] Recently, Kappe and coworkers have reported the development of sintered SiC microtiter plates for performing parallel synthesis in a multimode microwave reactor.[9] Considering the reactivity of *o*-quinol dimers and the available literature precedents, we wished to utilize SiC plates in a high-throughput reaction partner assessment.[10] In the current study, a broad panel of reaction partners in the retro-[4 + 2]/[4 + 2] cascade of *o*-quinol dimers have been evaluated under microwave conditions in an effort to study the scope and limitations of this methodology, to obtain both bicyclo[2.2.2]octenone and *cis*-decalin frameworks, and to understand the factors determining regio- and diastereoselectivity. To explain the observed reactivities and diastereoselectivities, in particular the regioselectivity for cycloadditions, computational studies of Diels–Alder reactions between *o*-quinols and select dienophiles/dienes were also conducted.[11] In this paper, we report the results of this study as well as biological screening of the resulting collection of complex cycloadducts.

Received: August 10, 2011
Published: September 26, 2011

Scheme 1. Synthesis of (+)-Chamaecypanone C Utilizing a Retro-[4 + 2]/[4 + 2] Cascade

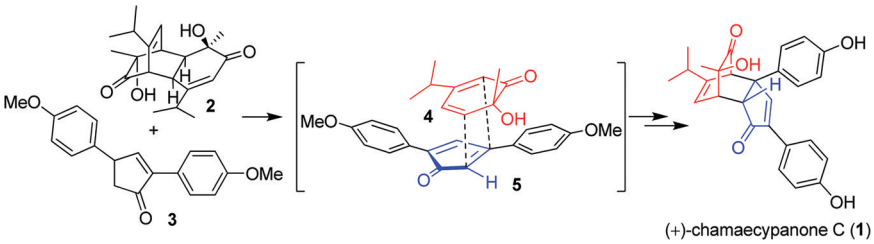

RESULTS AND DISCUSSION

Reaction Optimization. We first evaluated reactions between the readily accessible dimer (−)-**2**[12] and *N*-phenylmaleimide (**6**) under microwave conditions in various solvents (Table 1).[13] Although reactions went to completion within 30 min in either DMF (entry 1) or DMA (entry 2) to afford cycloadduct **7**, we noticed that use of mesitylene as solvent afforded cleaner reactions (entry 3). Further experiments (entry 4) indicated that reactions could be completed within 15 min (μW, 180 °C) in comparison to use of conventional heating (entry 5), which required approximately 90 min for completion.[2]

Table 1. Optimization of the Microwave-Mediated Retro-[4 + 2]/[4 + 2] Cascade

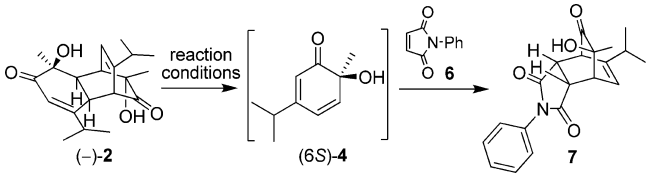

entry	solvent	conditions[a]	time (min)	conv[b] (%)
1	DMF	A	30	>99 (90)[c,d]
2	DMA	A	30	>99 (92)[d]
3	mesitylene	A	30	>99 (98)
4[e]	mesitylene	A	15	>99 (98)
5[f]	mesitylene	B	90	>99 (97)

[a]Reaction conditions: (A) 3.0 equiv of **6**, SiC chip, μW, 188 °C (IR temperature); (B) 3.0 equiv of *N*-phenylmaleimide (**6**), 150 °C. [b]Conversion based on UPLC analysis. [c]Isolated yield of product **7** in parentheses. [d]Aqueous workup required. [e]Reaction conducted at 180 °C (IR temperature) under microwave irradiation. [f]Reaction reported in ref 2.

Screening of Reaction Partners. Utilizing the optimized microwave conditions, 57 reaction partners were evaluated in a reaction screen (Figure 1).[13] A number of alkene partners were selected on the basis of retro-[4 + 2]/[4 + 2] cycloadditions of *o*-quinol dimers and MOB dimers reported in the literature.[1,3] Representative dipolarophiles and dienes were also included. Reactions were conducted on a 0.009 mmol scale using 3.0 mg of dimer (−)-**2** as substrate, 10 equiv of the corresponding reaction partner, and 100 μL of mesitylene under microwave irradiation at 180 °C (IR temp). After 60 min, reaction mixtures were filtered through a silica gel plug, concentrated, and evaluated using ultrahigh-performance liquid chromatography (UPLC)-MS, which allows for short analytical run times (approximately 3 min).[14] On the basis of UPLC-MS data, reactions showing major peaks in the HPLC trace were scaled up (0.06 mmol, 20 mg of substrate) using a SiC chip as passive heating element in a single-mode microwave reactor.[13] The results of the reaction screening indicated that dimer **2** was completely consumed in all cases. Of the 57 reactions, 12 afforded products corresponding to [4 + 2] adducts between the *o*-quinol and alkene reaction partners, and other reactions afforded product **8** (Scheme 2), likely generated from a dienone−phenol rearrangement of intermediate **4**.[15] The formation of **8** is in accordance with thermal degradation results reported in the literature for dimer **2**[16] and suggests that the corresponding reaction partners are unreactive in the cycloaddition event.

As shown in Table 2, *o*-quinol **4** may react with activated alkenes, including the normal-demand dienophiles MVK (**9a**), indene (**9b**), and 4-methoxystyrene (**9c**), the inverse-demand dienophiles dihydrofuran (DHF; **9d**) and vinylene carbonate (**9e**), and the alkynes dimethyl acetylenedicarboxylate (DMAD, **9f**) and phenylacetylene (**9g**). In all cases, Diels−Alder cycloaddition between *o*-quinol **4** and dienophiles **9** proceeded in a highly diastereoselective fashion with [4 + 2] adducts **10a−g** isolated in moderate to excellent yields. Structure elucidation of products using 2D NMR experiments or X-ray crystallography confirmed that endo-[4 + 2] cycloadducts were the predominate products isolated from the reactions,[13] which is in accordance with both experimental results and theoretical calculations in literature that secondary orbital overlap is believed to govern endo selectivity.[17] Facial selectivity could be explained by either steric or hyperconjugation effects according to our computational studies (vide infra).

In the cases of reaction with dienes (**11**, Table 3), *o*-quinol **4** was found to react as either a 4π or 2π reaction partner to afford the bicyclooctenone derivative **12** or *cis*-decalin product **13**. Reaction with the 1-phenyl-substituted 1,3-butadiene **11a** (entry 1) cleanly afforded a mixture of bicyclooctenones *endo*-**12a**α and *exo*-**12a**β in a 4:1 ratio favoring the endo adduct. When the 2-substituted 1,3-butadiene β-myrcene (**11b**, entry 2) was used in the reaction, *cis*-decalin **13b** was found to be the major product.[18] Considering the result that a mixture of two compounds was generated at lower reaction temperature (150 °C),[2] cycloadduct **13b** should be thermodynamically more favored in comparison to its bicyclooctenone isomer obtunone.[19] Similarly, reaction with 2,3-disubstituted 1,3-butadiene **11c** (entry 3) produced *cis*-decalin **13c** as the major product in excellent yield (94%). While reaction with cyclopentadiene dimer **11d** (entry 4) generated cycloadduct **12d** as the sole product in almost quantitative isolated yield, use of cyclohexadiene **11e** (entry 5) as a reaction partner led to a more complex product mixture. Structure elucidation confirmed that compounds **12e** and **13e** were the major products in this instance, along with a small amount of the rearranged bicyclooctene **14** (approximately 10%).

In order to probe possible interconversion between adducts **12e** and **13e**, pure compound **12e** was resubjected to the reaction conditions (μW, SiC, mesitylene, 180 °C, 15 min).

dx.doi.org/10.1021/jo201658y | J. Org. Chem. 2011, 76, 8944−8954

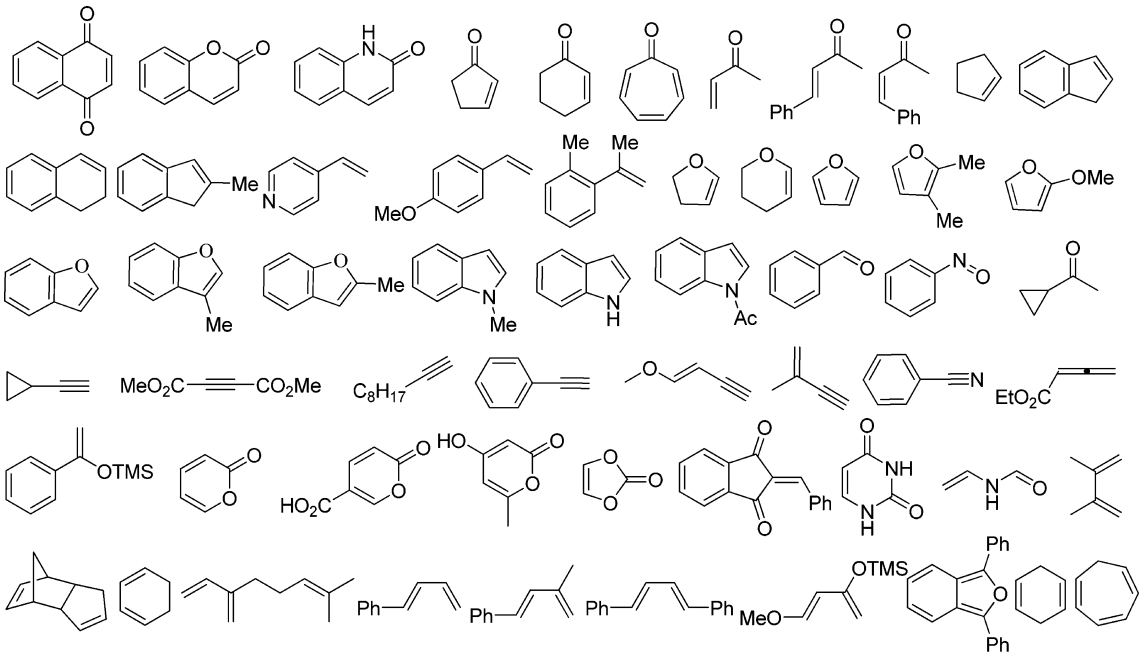

Figure 1. Reaction partners for retro-[4 + 2]/[4 + 2] cascade.

Scheme 2. Dienone–Phenol Rearrangement of *o*-Quinol 4

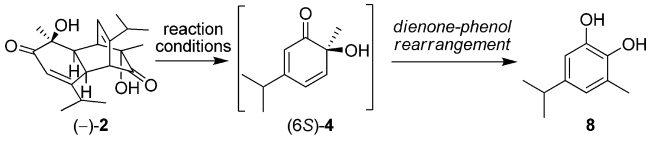

Product analysis indicated that a mixture of cycloadducts **12e**, **13e**, and **14** was generated in a 2:1:1 ratio. An extended reaction time (1 h) or elevated temperature (200 °C) did not change the ratio, in which case further decomposition was observed. It is plausible that compounds **12e** and **13e** may interconvert through Cope rearrangement[20] (Figure 2, pathway a) or via a retro-[4 + 2] reaction of **12e** followed by recombination of *o*-quinol and cyclohexadiene (pathway b). To further understand this process, trapping experiments were conducted as shown in Scheme 3. In both experiments, no crossover Diels–Alder cycloadduct was observed; reactions afforded either a mixture of **12e**/**13e**/**14** from **12e** or recovered starting materials from cycloadduct **7**. These results support an intramolecular [3,3]-sigmatropic rearrangement mechanism for the interconversion of cycloadducts **12e** and **13e**.[21]

The generation of product **14** may be explained by thermal α-ketol rearrangement of hydroxy enone **13e** (Figure 2, pathway c).[22] A similar ring contraction has been observed in a related α-methyl-α-hydroxylcyclohexanone system under basic conditions.[23] However, use of related basic conditions (LiHMDS/THF or Al_2O_3/hexanes) did not effect ketol rearrangement of **13e.**

On the basis of the results from our reaction screen and follow-up product analyses, we noticed that activated alkenes or alkynes are more reactive in the reaction with the model *o*-quinol. Moreover, *cis*-alkenes in general showed better reactivity than *trans*-alkenes and 1,1-disubstituted and trisubstituted alkenes. Acyclic 1,3-dienes were found to react as 4π components only if they lacked substitution at the C1 or C4 positions and displayed reactivity as 2π components in the cases of less substituted alkenes. Taken together, these results suggest that Diels–Alder cycloaddition of *o*-quinols is an electronically and sterically demanding process. These observations are also in accordance with examples of 2,4-cyclohexadienones reported in the literature.[1,3]

To further evaluate the scope of the microwave-assisted protocol, *o*-quinol dimers (+)-**15**,[12] **16**,[24] **17**, and **18**[25] were subjected to optimized reaction conditions (μW, SiC, mesitylene, 170 °C, 15 min, Table 4). In all cases, good to excellent isolated yield of the desired cycloadducts **19–25** were obtained as single diastereomers.

Computational Studies. Previously computational modeling has been employed mainly in studies of MOBs as dienes in [4 + 2] cycloadditions.[3a,26] Quideau and co-workers have also utilized calculations to study the dimerization of *o*-quinols.[27] We wished to further study Diels–Alder cycloadditions of *o*-quinols and dienophiles/dienes computationally to further understand the energetics and regio- and stereochemical features of the cycloadditions.

In our studies, B3LYP calculations[28] first showed (Table 5, entry 1) that cycloreversion of dimer **2** is modestly endothermic, with forward and reverse barriers of 23.9 and 12.3 kcal/mol, respectively. The lowest energy transition state has C_2 symmetry; similar results have been described for related cycloadditions.[25] Predicted reaction energetics support a low transient concentration of dienone **4**. Cycloaddition of **4** with **9a,d,b** as representative dienophiles is predicted in each case (entries 2–4) to have a low reaction barrier, with exothermicity favorable to a unidirectional process. For each of these reactions, we optimized all *eight* potential transition states; the observed product was correctly assigned by theory in all cases. In every favored cycloaddition, the shorter transition-state bond connects to C-5 of dienone **4** (Figure 3). Two failed reactants, **27** and **28**, showed unexpectedly higher reaction barriers (entries 6 and 7) in comparison to structural analogues **9a,b**. It is noteworthy that the barriers for two reaction modes of myrcene (**11b**, entry 5) are nearly equal, consistent with the experimental product distribution (ca. 1:1) at lower reaction temperature (150 °C).[2] The lower energy **13b** was the sole

dx.doi.org/10.1021/jo201658y | *J. Org. Chem.* 2011, 76, 8944–8954

Table 2. Retro-[4 + 2]/[4 + 2] Reactions To Afford Bicyclo[2.2.2]octenones[a]

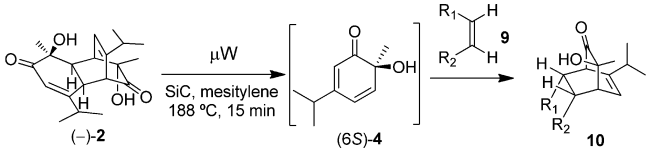

entry	dienophile (equiv)	cycloadduct[b]	yield[c] (%)
1	 (5 equiv) **9a**	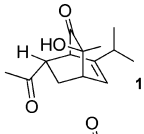 **10a**	85
2	 (10 equiv) **9b**	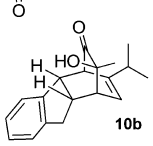 **10b**	99
3	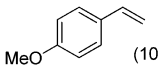 (10 equiv) **9c**	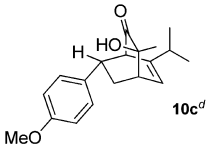 **10c**[d]	98
4	 (20 equiv) **9d**	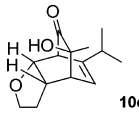 **10d**	85
5	 (20 equiv) **9e**	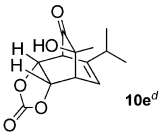 **10e**[d]	76
6	MeO_2C—≡—CO_2Me (10 equiv) **9f**	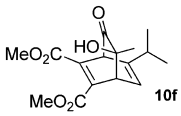 **10f**	90
7	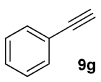 **9g** (10 equiv)	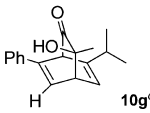 **10g**[d]	80

[a]Reaction conditions: dimer (−)-**2**, dienophile, SiC chip, mesitylene, μW, 180 °C, 15 min. [b]Single diastereomer isolated unless otherwise noted. [c]Isolated yield after column chromatography. [d]Approximately 9% of an inseparable minor product observed by ^{1}H NMR (ca. 10:1 isomeric ratio).

product generated from the reaction at higher temperature (180 °C; cf. Table 3, entry 2), presumably from cycloadduct **26** via Cope rearrangement.

The observed ensemble of selectivity and the correlation between theory and experiment are striking. In all cases, cycloaddition stereochemistry favors the usual Alder endo rule, with additional facial selectivity syn to the less sterically demanding hydroxyl group. Hyperconjugative effects (Cieplak–Fallis model)[29] from the methyl group in the transition state may also contribute to facial selectivity.[25,30] Dienone **4** has a high-lying HOMO (−6.9 eV) and a low-lying LUMO (−2.3 eV) and as a consequence reacts with both electron-rich and electron-poor dienophiles. In every case, the preferred regiochemistry follows initial bonding to C5 of the dienone, which maximizes resonance stabilization in the asynchronous

Table 3. Retro-[4 + 2]/[4 + 2] Cycloadditions with Dienes[a]

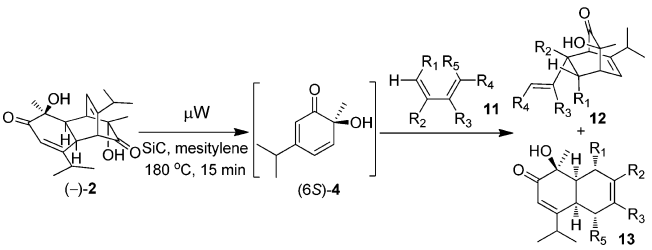

entry	dienophile (equiv)	cycloadduct	yield[b] (%)
1	 (10 equiv) **11a**	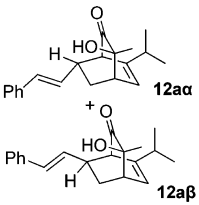 **12aα** + **12aβ**	81 + 18
2	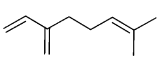 **11b** (10 equiv)	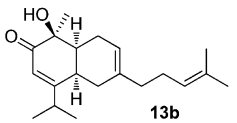 **13b**	57
3	 (10 equiv) **11c**	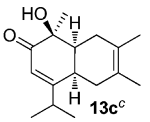 **13c**[c]	94
4	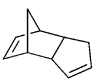 (5 equiv) **11d**	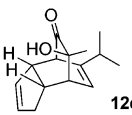 **12d**	98
5	 (20 equiv) **11e**	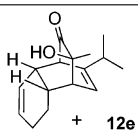 **12e** + 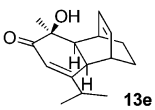 **13e** + 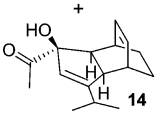 **14**	57 + 25 + 9

[a]Reaction conditions: dimer (−)-**2**, diene, SiC chip, mesitylene, μW, 180 °C, 15 min. [b]Isolated yield after column chromatography. [c]Approximately 5% of an inseparable minor product was observed by ^{1}H NMR analysis (ca. 19:1 isomeric ratio).

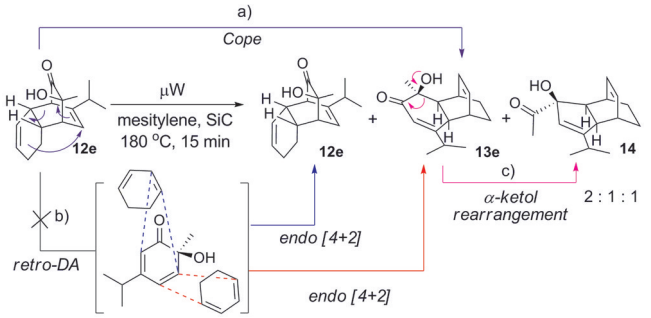

Figure 2. Cope rearrangement vs a retro-[4 + 2]/[4 + 2] process.

dx.doi.org/10.1021/jo201658y | J. Org. Chem. 2011, 76, 8944–8954

Scheme 3. Trapping Experiment

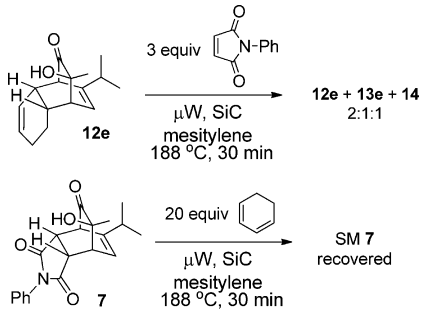

Table 4. Retro-[4 + 2]/[4 + 2] Cascade Using Other *o*-Quinol Precursors[a]

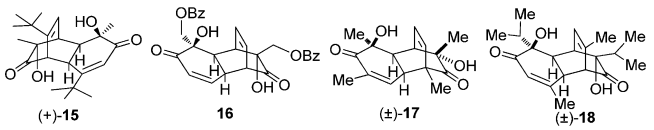

entry	dimer	dienophile (equiv)	cycloadduct[b]	yield[c] (%)
1	(+)-**15**	(5 equiv) **11d**	**19**	93
2	(+)-**15**	(20 equiv) **9e**	**20**	78
3	**16**	(10 equiv) **9b**	**21**	86
4	(±)-**17**	(3 equiv) **6**	**22**	99
5	(±)-**17**	(10 equiv) **9b**	**23**	78
6	(±)-**17**	(20 equiv) **9d**	**24**	85
7	(±)-**18**	(3 equiv) **6**	**25**	80

[a]Reaction conditions: dimer, dienophile, SiC chip, mesitylene, μW, 170 °C, 15 min. [b]Single diastereomer isolated. [c]Isolated yield after silica gel chromatography.

transition state. In general, reactions with lower barriers showed more asynchronous transition-state structures.[31]

In a side by side comparison of MVK (**9a**) and cyclopentenone **27**, electronically similar dienophiles, the MVK π system shows better secondary orbital overlap in transition states in reactions with *o*-quinol **4** (Figure 3, TS2). In contrast, the exo C═O double bond of cyclic ketone **27** does not align well with the *o*-quinol in the transition state (TS6). Similarly, in

Table 5. B3LYP/6-31G(d) Reaction Energetics

entry	reactant(s)	transition state	product(s)
1	(−)-**2**	**TS1** 23.9	2 × **(6S)-4** 11.6
	E_{rel} = 0.0 kcal/mol		
2	**(6S)-4** + **9a**	**TS2** 13.8	**10a** -17.3
	E_{rel} = 0.0 kcal/mol		
3	**(6S)-4** + **9d**	**TS3** 17.0	**10d** -18.5
	E_{rel} = 0.0 kcal/mol		
4	**(6S)-4** + **9b**	**TS4** 17.8	**10b** -14.9
	E_{rel} = 0.0 kcal/mol		
5	**(6S)-4** + **11b**	**TS5a** 17.5	**13b** -26.9
	E_{rel} = 0.0 kcal/mol	**TS5b** 16.9	**26** -13.7
6	**(6S)-4** + **27**	**TS6** 23.5	**29** -13.4
	E_{rel} = 0.0 kcal/mol		
7	**(6S)-4** + **28**	**TS7** 22.9	**30** -10.3
	E_{rel} = 0.0 kcal/mol		

TS4 the arene has a more optimal $\pi-\pi$ interaction with the 4π partner, while in TS7 the dihydronaphthalene (**28**) aromatic ring is oriented nearly perpendicular to the cyclohexadienone ring, presumably to minimize steric interactions, thereby raising TS energetics by 5.1 kcal/mol in comparison to the indene case (cf. Table 5, entries 4 and 7). In addition to the sterics and electronics of dienophiles, these results suggest that secondary orbital overlap of dienophiles with *o*-quinols may be another important factor determining dienophile reactivity.

Competition between cycloreversion, [3,3]-sigmatropic shifts[20,21] and secondary dienone−phenol[32] or α-ketol[22] rearrangements add complexity to these results. For example, DFT calculations show that (−)-**2** should undergo a degenerate and homochiral Cope rearrangement with a barrier of 22.4 kcal/mol which should compete with cycloreversion. Figure 4 summarizes the predicted energetics for the dienone **4** + 1,3-cyclohexadiene potential surface. No transition state for [4 + 2] cycloaddition leading directly to **13e** (**TS9**) was identified with DFT calculations. Repeated attempts to locate **TS9** instead optimized to **TS8**, which leads to **12e**. On the basis of these predictions, the most likely pathway to **13e** is through a Cope rearrangement of **12e** which has a predicted barrier of 29.6 kcal/mol. According to their relative energetics, Cope

dx.doi.org/10.1021/jo201658y | J. Org. Chem. 2011, 76, 8944–8954

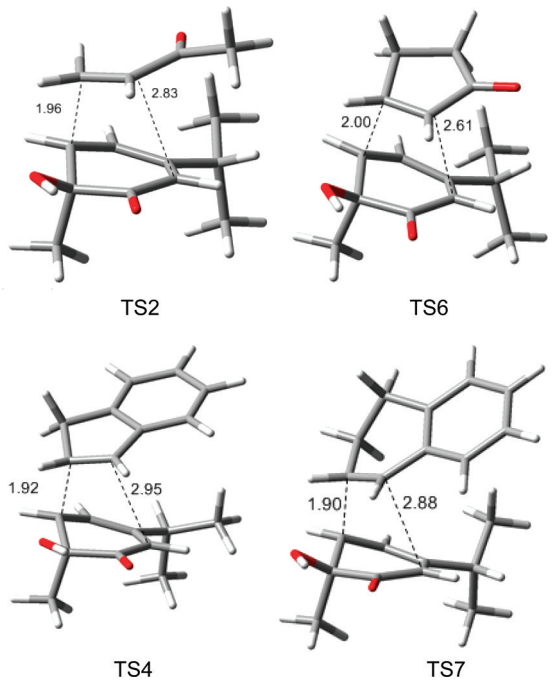

Figure 3. Examples of transition-state structures.

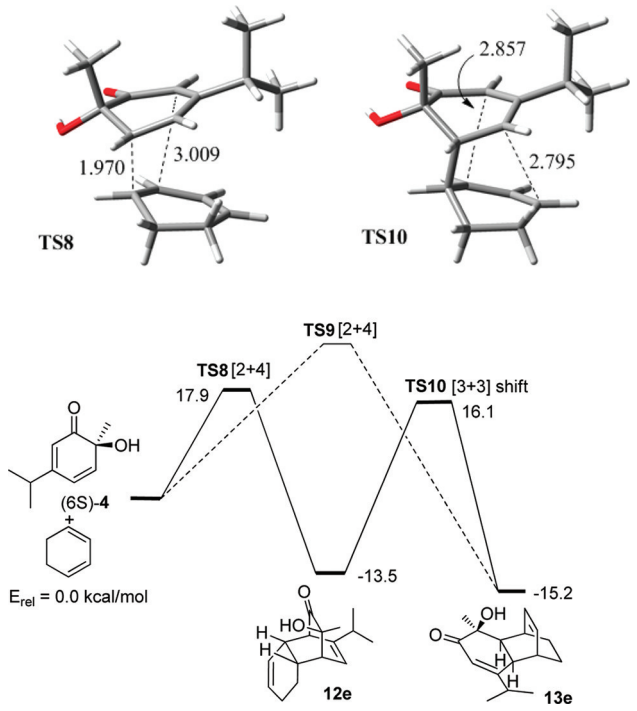

Figure 4. DFT results for cycloaddition and Cope rearrangement.

rearrangement of **12e** should be favored over cycloreversion. Our trapping experiments (Scheme 3) supported only a [3,3]-sigmatropic rearrangement for interconversion of **12e** and **13e**, consistent with computations.

The rearrangement of **13e** to **14** can proceed by thermal isomerization of neutral **13e** or through catalysis by acid, base, or lithiation. Computational results are summarized in Scheme 4. The predicted thermal barrier (41.1 kcal/mol) is too high to be operative. Protonation, deprotonation, or lithiation of **13e** all decrease the predicted barrier significantly and affect product

Scheme 4. DFT Results for α-Ketol Rearrangement Pathways

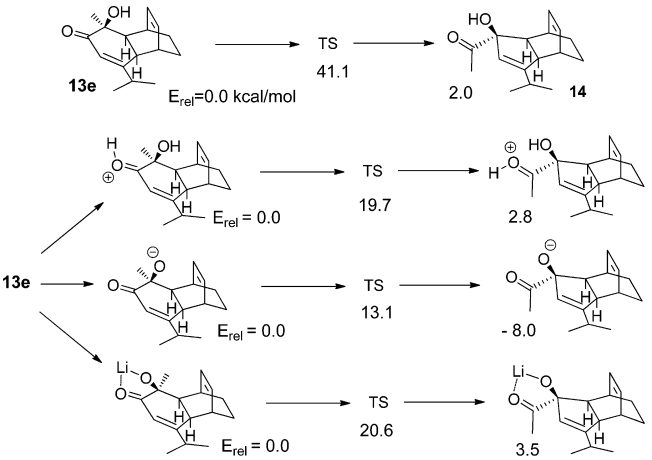

energetics. Adventitious proton catalysis seems most compatible with our experimental results. For the most favorable case, B3LYP/6-31+G(d) calculations predict that deprotonated **13e** should undergo an exothermic rearrangement with a barrier of only 13.1 kcal/mol. The apparent conflict of this result with our LiHMDS-catalyzed experiments (vide infra) was resolved by showing that rearrangement of lithiated **13e** is now endothermic by 3.5 kcal/mol because O–Li–O bridging creates product strain.

Rearrangement of **4** to **8** can proceed by similarly diverse mechanisms.[22,32] DFT computations for the methyl migration step (Scheme 5) showed low barriers for ionic pathways. Once again, our experimental results are consistent with trace acid catalysis.

Biological Studies. Both enantiomers of synthesized bicyclo[2.2.2]octenones and *cis*-decalins were subjected to screening at 20 μM for inhibition in three biological assays at the National Cancer Institute (NCI): AP-1 (activator protein-1, an oncogenic transcription factor),[33] TRAIL (tumor necrosis factor-α-related apoptosis-inducing ligand) sensitization,[34] and HIF-2 (hypoxia inducible factor 2).[35] Compound (−)-**31** (Figure 5, inset) showed selective inhibition against AP-1 at 4 μM concentration with luciferase reporter assays in HEK293 cells. TPA (12-*O*-tetradecanoylphorbol-13-acetate) induced AP-1 activity was repressed by more than 50% after pretreatment with the compound at 8 μM. However, the compound did not show inhibition of NF-κB (nuclear factor kappa B) or SRE (serum response element) dependent transcription at the same concentration (Figure 5). SRE was also used as a proliferation control which can measure cytotoxic activity for the compound. Thus, this result suggests that compound (−)-**31** targets the events needed for AP-1 activation selectively, rather than other transcription factors such as HIF-2, NF-κB, and SRE. As AP-1 is required for tumor promotion and progression,[36] identification of novel and specific AP-1 inhibitors such as bicyclooctenone (-)-**31** may be beneficial for cancer prevention and therapy. Although further experiments in the NCI 60-cell screen at 10 μM showed that (−)-**31** did not pass the threshold for further evaluation of cell growth inhibition, analogues of compound **31** may be pursued in future studies for SAR analysis.

dx.doi.org/10.1021/jo201658y | *J. Org. Chem.* 2011, 76, 8944–8954

Scheme 5. DFT Results for Dienone–Phenol Rearrangement

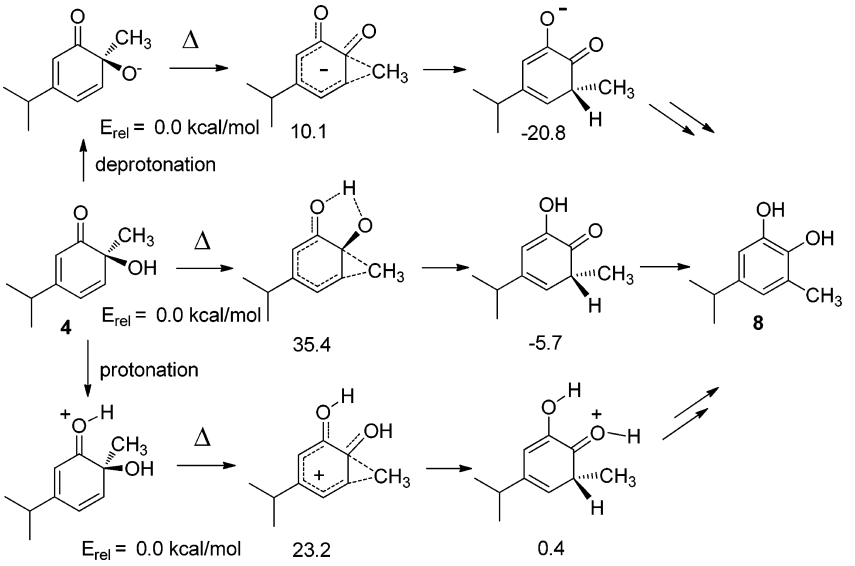

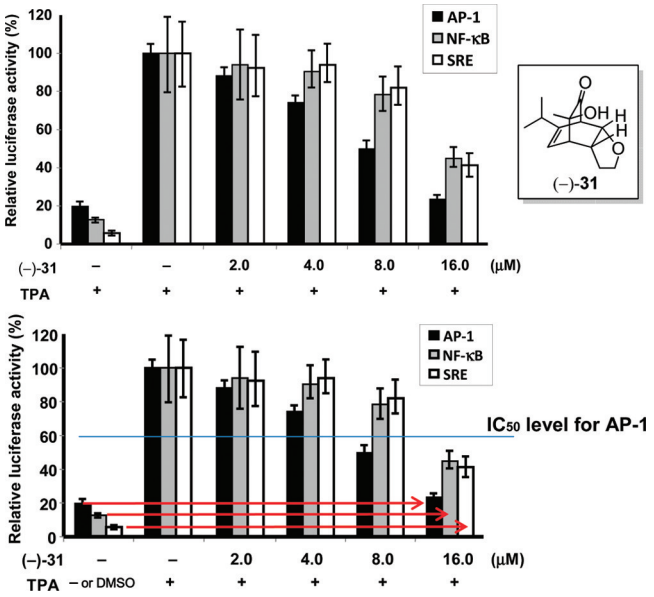

Figure 5. (–)-**31** shows higher selectivity for AP-1-dependent activity than other transcription factors.

CONCLUSION

We have utilized microwave-assisted parallel screening for evaluation of Diels–Alder reactions of *o*-quinol dimers in an effort to identify reactive reaction partners among a broad panel of compounds. Elucidation of products, analysis of the results, and computational studies allowed us to not only confirm the diastereoselectivity of [4 + 2] cycloadditions of *o*-quinols but also determine that sterics and proper secondary orbital alignment are the major governing factors for dienophile reactivity. The high concordance between experimental and calculated results suggest that theoretical calculations of energetics may be used to prescreen reaction partners for [4 + 2] cycloadditions of *o*-quinols.[37] Furthermore, biological evaluation of a set of compounds generated in the study showed that bicyclo[2.2.2]octenones may be worthwhile scaffolds for development of screening libraries, as novel AP-1 inhibitory activity was observed for one member of the small library. Further studies involving retro-Diels–Alder/Diels–Alder cascade processes to produce natural products and analogues are currently in progress and will be reported in future publications.

EXPERIMENTAL SECTION

Optimization of the Retro-[4 + 2]/[4 + 2] Reaction. A 10 mL microwave tube with a silicon carbide chip was charged with dimer **2** (10.0 mg, 0.030 mmol) and *N*-phenylmaleimide (**6**; 15.6 mg, 0.150 mmol).[13] A 0.5 mL amount of solvent was added under an argon atmosphere and the reaction was irradiated in a microwave reactor (stir off) at the indicated temperature (cf. Table 1). Reactions in DMF (entry 1) and DMA (entry 2) were directly submitted to UPLC-MS analysis, and crude reaction mixtures were diluted with EtOAc, washed with water and brine, and dried over $MgSO_4$. The organic fraction was concentrated, dried in vacuo, and purified by silica gel column chromatography. Reactions in mesitylene were stopped after the indicated reaction time, and the crude mixture was passed through a short silica gel plug, flushed using hexanes to remove mesitylene, and finally flushed with EtOAc to elute both the product and excess maleimide **6**. The organic fraction was concentrated, dried in vacuo, analyzed by UPLC-MS, and purified by silica gel column chromatography to afford cycloadduct **7**.

Reaction Partner Screening. In a microwave reaction vessel (4 × 48 well SiC block) were charged dimer **2** (3.0 mg, 0.009 mmol), dienophiles/dienes (10 equiv), and 100 μL of mesitylene.[13] The resulting mixtures were heated in a microwave reactor with a 48-well SiC block (stir off) at 180 °C (IR temperature) for 1 h. After the reaction, the crude mixture was passed through a short silica gel plug, flushed using hexanes to remove mesitylene, and finally flushed with EtOAc to elute both the product and excess dienophiles/dienes. The organic fraction was finally concentrated and analyzed by UPLC-MS.

General Procedure for Microwave Reaction of *o*-Quinol Dimers (20–30 mg Scale). A 10 mL microwave tube with a silicon carbide chip was charged with *o*-quinol dimer (0.060 mmol) and dienophile (equivalents, cf. Tables 2–4). A 0.5 mL portion of mesitylene was added under an argon atmosphere, and the reaction mixture was irradiated in a microwave reactor at 170 or 180 °C (IR temperature) for 15 min (stir off). Reactions were stopped after the indicated reaction time, and the crude mixture was passed through a short silica gel plug, flushed using hexanes to remove mesitylene (and in a few cases excess nonpolar dienophiles), and finally flushed with EtOAc to elute the crude products. The organic fraction was concentrated and dried in vacuo, and the residue was purified by

dx.doi.org/10.1021/jo201658y | *J. Org. Chem.* 2011, 76, 8944–8954

silica gel column chromatography to afford the corresponding Diels–Alder adducts.

(1*R*,3*S*,4*S*,7*S*)-3-Hydroxy-7-(4-methyoxy)phenyl-3-methyl-6-(propan-2-yl)bicyclo[2.2.2]oct-5-en-2-one (10c). Dimer **2** (20.0 mg, 0.060 mmol) and 4-vinylanisole (**9c**; 81.0 μL, 0.60 mmol) were thermolyzed by following the general procedure. The crude mixture was purified by silica gel chromatography (hexanes/EtOAc 10/1 to 8/1) followed by preparative TLC (CH_2Cl_2/EtOAc 10/1) to afford product **10c** (35.5 mg, 98%) as a yellow oil: R_f = 0.41 (hexanes/EtOAc 2/1); IR (thin film) ν_{max} 3434, 2959, 1721, 1511, 1248, 1178 cm^{-1}; ^1H NMR ($CDCl_3$, 400 MHz) δ 7.07 (d, J = 8.0 Hz, 2H), 6.79 (d, J = 8.0 Hz, 2H), 6.18 (d, J = 7.2 Hz, 1H), 3.77 (s, 3H), 3.38 (dd, J = 8.4, 5.6 Hz, 1H), 3.06 (d, J = 0.8 Hz, 1H), 2.94 (ddd, J = 6.0, 3.2, 2.4 Hz, 1H), 2.68 (ddd, J = 12.8, 9.6, 2.4 Hz, 1H), 2.53 (s, 1H), 1.90 (sept, J = 6.8 Hz, 1H), 1.61 (ddd, J = 12.8, 6.0, 2.8 Hz, 1H), 1.28 (s, 3H), 0.89 (d, J = 6.8 Hz, 3H), 0.73 (d, J = 6.8 Hz, 3H); ^{13}C NMR ($CDCl_3$, 100 MHz) δ 213.0, 158.4, 144.7, 135.9, 128.7 (two carbons overlapping), 125.7, 113.6 (two carbons overlapping), 72.1, 59.0, 55.2, 43.1, 39.9, 33.1, 27.6, 25.9, 20.5, 19.7; HRMS-ESI (m/z) $[M - H_2O + H]^+$ calcd for $C_{19}H_{23}O_2$ 283.1698, found 283.1713; $[\alpha]^{22}_D$ = +36.4° (c = 0.67, $CHCl_3$).

(1*R*,2*S*,6*R*,7*S*,9*S*)-9-Hydroxy-9-methyl-11-(propan-2-yl)-3,5-dioxatricyclo[5.2.2.0^{2,6}]undec-10-ene-4,8-dione (10e). Dimer **2** (20.0 mg, 0.060 mmol) and vinylene carbonate (**9e**; 77.3 μL, 1.20 mmol) were thermolyzed by following the general procedure. The crude mixture was purified by silica gel chromatography (hexanes/EtOAc 3/1) to afford product **10e** (23.1 mg, 76%) as a white solid: R_f = 0.11 (hexanes/EtOAc 3/1); mp 135–137 °C; IR (thin film) ν_{max} 3426, 2964, 1795, 1731, 1164, 1057 cm^{-1}; ^1H NMR ($CDCl_3$, 400 MHz) δ 5.97 (d, J = 6.4 Hz, 1H), 5.36 (dd, J = 8.0, 3.6 Hz, 1H), 5.04 (dd, J = 8.0, 3.6 Hz, 1H), 3.64 (dd, J = 3.6, 2.0 Hz, 1H), 3.38 (dd, J = 6.4, 3.6 Hz, 1H), 2.43 (s, 1H), 2.39 (sept, J = 6.8 Hz, 1H), 1.32 (s, 3H), 1.022 (d, J = 6.8 Hz, 3H), 1.016 (d, J = 6.8 Hz, 3H); ^{13}C NMR ($CDCl_3$, 100 MHz) δ 205.5, 154.4, 145.5, 122.2, 74.6, 74.3, 71.9, 54.4, 45.8, 33.1, 25.2, 20.23, 20.18; HRMS-ESI (m/z) $[2M + Na]^+$ calcd for $C_{26}H_{32}NaO_{10}$ 527.1893, found 527.1880; $[\alpha]^{22}_D$ = +125.6° (c = 0.52, $CHCl_3$).

(1*R*,4*S*,7*S*)-Dimethyl-7-hydroxy-7-methyl-8-oxo-5-(propan-2-yl)bicyclo[2.2.2]octa-2,5-diene-2,3-dicarboxylate (10f). Dimer **2** (20.0 mg, 0.060 mmol) and dimethyl acetylenedicarboxylate (**9f**; 74.0 μL, 0.60 mmol) in 300 μL of mesitylene were thermolyzed by following the general procedure. The crude mixture was purified by silica gel chromatography (CH_2Cl_2/EtOAc 15/1 to 10/1) to afford product **10f** (33.3 mg, 90%) as a yellow oil: R_f = 0.30 (CH_2Cl_2/EtOAc 5/1); IR (thin film) ν_{max} 3485, 2959, 1726, 1265 cm^{-1}; ^1H NMR ($CDCl_3$, 400 MHz) δ 6.03 (d, J = 6.4 Hz, 1H), 4.35 (d, J = 2.0 Hz, 1H), 4.04 (d, J = 6.0 Hz, 1H), 3.81 (s, 3H), 3.77 (s, 3H), 2.54 (s, 1H), 2.48 (doublet of sept, J = 6.8, 1.2 Hz, 1H), 1.32 (s, 3H), 1.02 (d, J = 6.8 Hz, 6H); ^{13}C NMR ($CDCl_3$, 100 MHz) δ 201.9, 166.4, 164.2, 149.8, 143.2, 134.4, 123.7, 67.4, 58.1, 52.7, 52.6, 50.8, 31.9, 26.3, 20.3 (two carbons overlapping); HRMS-ESI (m/z) $[M + Na]^+$ calcd for $C_{16}H_{20}NaO_6$ 331.1158, found 331.1158; $[\alpha]^{22}_D$ = +58.7° (c = 0.51, $CHCl_3$).

(1*S*,3*S*,4*R*)-3-Hydroxy-3-methyl-6-phenyl-7-(propan-2-yl)-bicyclo[2.2.2]octa-5,7-dien-2-one (10g). Dimer **2** (20.0 mg, 0.060 mmol) and vinylene carbonate (**9g**; 65.9 μL, 1.20 mmol) were thermolyzed by following the general procedure. The crude mixture was purified by silica gel chromatography (hexanes/EtOAc 8/1) to afford product **14** (25.8 mg, 80%) as a yellow oil: R_f = 0.27 (hexanes/EtOAc 3/1); IR (thin film) ν_{max} 3434, 2963, 1724, 1445, 1068 cm^{-1}; ^1H NMR ($CDCl_3$, 400 MHz) δ 7.46–7.44 (m, 2H), 7.36–7.32 (m, 2H), 7.29–7.26 (m, 1H), 6.73 (dd, J = 6.0, 2.0 Hz, 1H), 6.08 (dd, J = 6.4, 2.0 Hz, 1H), 4.43 (dd, J = 2.0, 2.0 Hz, 1H), 3.79 (ddd, J = 6.4, 6.4, 2.0 Hz, 1H), 2.53 (sept, J = 6.8 Hz, 1H), 2.30 (s, 1H), 1.35 (s, 3H), 1.07 (d, J = 6.8 Hz, 3H), 1.05 (d, J = 6.8 Hz, 3H); ^{13}C NMR ($CDCl_3$, 100 MHz) δ 205.3, 149.2, 141.1, 136.0, 129.2, 128.6 (two carbons overlapping), 127.8, 125.3 (two carbons overlapping), 125.1, 69.5, 60.3, 48.5, 32.1, 26.4, 20.7 (two carbons overlapping); HRMS-ESI (m/z) $[M + Na]^+$ calcd for $C_{18}H_{20}NaO_2$ 291.1361, found 291.1363; $[\alpha]^{22}_D$ = +27.6° (c = 0.81, $CHCl_3$).

(1*R*,3*S*,4*S*,7*R*)-3-Hydroxy-3-methyl-7-[(*E*)-2-phenylethenyl]-6-(propan-2-yl)bicyclo[2.2.2]oct-5-en-2-one (12a*α*). Dimer **2** (20.0 mg, 0.120 mmol) and 1-phenyl-1,3-butadiene[38] (**11a**; 76.1 mg, 1.20 mmol) were thermolyzed by following the general procedure. The crude mixture was purified by preparative TLC (hexanes/EtOAc 4/1) to afford product **12a*α*** (28.8 mg, 81%) as a white solid: R_f = 0.22 (hexanes/EtOAc 5/1); mp 68–70 °C; IR (thin film) ν_{max} 3439, 2962, 2932, 1725, 1449, 1126 cm^{-1}; ^1H NMR ($CDCl_3$, 500 MHz) δ 7.27–7.26 (m, 4H), 7.20–7.17 (m, 1H), 6.37 (dd, J = 16.0, 1.0 Hz, 1H), 6.11 (ddd, J = 7.0, 1.5, 1.5 Hz, 1H), 5.86 (dd, J = 16.0, 8.5 Hz, 1H), 3.09 (dd, J = 2.0, 2.0 Hz, 1H), 3.00–2.94 (m, 1H), 2.83 (ddd, J = 7.0, 3.0, 2.5 Hz, 1H), 2.53 (ddd, J = 12.5, 8.5, 3.0 Hz, 1H), 2.50 (bs, 1H), 2.30 (doublet of sept, J = 7.0, 1.0 Hz, 1H), 1.26 (s, 3H), 1.21 (ddd, J = 13.0, 5.0, 2.5 Hz, 1H), 1.02 (d, J = 7.0 Hz, 3H), 0.98 (d, J = 7.0 Hz, 3H); ^{13}C NMR ($CDCl_3$, 100 MHz) δ 212.9, 144.4, 137.1, 132.6, 129.7, 128.5 (two carbons overlapping), 127.2, 126.2, 126.0 (two carbons overlapping), 72.3, 56.6, 42.9, 39.2, 33.1, 27.3, 25.9, 20.9, 20.5; HRMS-ESI (m/z) $[M - H_2O + H]^+$ calcd for $C_{20}H_{23}O$ 279.1749, found 279.1748; $[\alpha]^{22}_D$ = +119.5° (c = 0.91, $CHCl_3$).

(1*R*,3*S*,4*S*,7*S*)-3-Hydroxy-3-methyl-7-[(*E*)-2-phenylethenyl]-6-(propan-2-yl)bicyclo[2.2.2]oct-5-en-2-one (12a*β*). Utilizing the same protocol as for compound **12a*α***, product **12a*β*** (19.8 mg, 97%) was isolated as a white solid: R_f = 0.32 (hexanes/EtOAc 5/1); mp 104–106 °C; IR (thin film) ν_{max} 3440, 2962, 2871, 1726, 1449, 1142, 1081 cm^{-1}; ^1H NMR ($CDCl_3$, 400 MHz) δ 7.33–7.26 (m, 4H), 7.21–7.17 (m, 1H), 6.40 (d, J = 15.6 Hz, 1H), 6.10 (ddd, J = 15.6, 8.8, 1.6 Hz, 1H), 6.04 (dd, J = 6.8, 1.2 Hz, 1H), 3.03 (dd, J = 1.6, 1.6 Hz, 1H), 2.85–2.82 (m, 1H), 2.65–2.58 (m, 1H), 2.40 (sept, J = 6.8 Hz, 1H), 2.30 (s, 1H), 2.12 (ddd, J = 12.8, 5.2, 2.0 Hz, 1H), 1.77–1.70 (m, 1H), 1.28 (s, 3H), 1.05 (d, J = 6.8 Hz, 3H), 1.04 (d, J = 6.8 Hz, 3H); ^{13}C NMR ($CDCl_3$, 100 MHz) δ 213.4, 147.8, 137.1, 132.1, 130.3, 128.5 (two carbons overlapping), 127.2, 126.3 (two carbons overlapping), 125.5, 73.5, 56.6, 43.1, 42.5, 32.6, 26.4, 26.3, 20.54, 20.50; HRMS-ESI (m/z) $[M + H]^+$ calcd for $C_{20}H_{25}O_2$ 297.1855, found 297.1867; $[\alpha]^{22}_D$ = +137.8° (c = 0.57, $CHCl_3$).

(1*S*,4a*R*,8a*S*)-1-Hydroxy-1-methyl-6-(4-methylpent-3-en-1-yl)-4-(propan-2-yl)-4a,5,8,8a-tetrahydronaphthalen-2(1*H*)-one (13b). Dimer **2** (20.0 mg, 0.060 mmol) and *β*-myrcene **11c** (103.3 μL, 0.60 mmol) were thermolyzed by following the general procedure. The crude mixture was purified, and **13b** was isolated as a colorless oil (20.8 mg, 57%). ^1H NMR, ^{13}C NMR, and IR spectra for compound **13b** were found to be identical with those reported in the literature:[17] R_f = 0.38 (hexanes/EtOAc 5/1); $[\alpha]^{22}_D$ = +217.9° (c = 1.01, $CHCl_3$).

(1*S*,4a*R*,8a*S*)-1-Hydroxy-1,6,7-trimethyl-4-(propan-2-yl)-4a,5,8,8a-tetrahydronaphthalen-2(1*H*)-one (13c). Dimer **2** (20.0 mg, 0.060 mmol) and 2,3-dimethyl-1,3-butadiene (**11c**; 67.9 μL, 0.60 mmol) were thermolyzed by following the general procedure. The crude mixture was purified by silica gel chromatography (hexanes/EtOAc 20/1 to 15/1) to afford product **13c** (27.3 mg, 92%) as an oil: R_f = 0.38 (hexanes/EtOAc 8/1); IR (thin film) ν_{max} 3491, 2968, 2926, 1722, 1671, 1242, 1152 cm^{-1}; ^1H NMR ($CDCl_3$, 400 MHz) δ 5.85 (d, J = 2.8 Hz, 1H), 3.55 (s, 1H), 2.94–2.91 (m, 1H), 2.38 (sept, J = 6.8 Hz, 1H), 2.35–2.30 (m, 3H), 2.07 (dd, J = 17.6, 6.8 Hz, 1H), 1.59 (s, 3H), 1.48 (s, 3H), 1.32 (s, 3H), 1.06 (d, J = 6.8 Hz, 3H), 1.01 (d, J = 6.8 Hz, 3H); ^{13}C NMR ($CDCl_3$, 100 MHz) δ 203.1, 172.8, 126.1, 123.3, 120.0, 76.6, 44.4, 36.8, 33.3, 30.8, 29.4, 24.4, 22.4, 20.6, 19.0, 18.7; HRMS-ESI (m/z) $[M + H]^+$ calcd for $C_{16}H_{24}O_2$ 249.1855, found 249.1876; $[\alpha]^{22}_D$ = +133.6° (c = 0.46, $CHCl_3$).

(1*S*,2*R*,7*S*,8*R*,10*S*)-10-Hydroxy-10-methyl-12-(propan-2-yl)-tricyclo[6.2.2.0^{2,7}]dodeca-5,11-dien-9-one (12e). Dimer **2** (60.0 mg, 0.180 mmol) and 1,3-cyclohexadiene (**11e**; 343.0 μL, 3.60 mmol) were thermolyzed by following the general procedure. The crude mixture was purified by silica gel chromatography (hexanes/EtOAc 20/1 to 15/1) to afford **12e** (51.8 mg, 57%) as a white solid: R_f = 0.32 (hexanes/EtOAc 5/1); mp 46–48 °C; IR (thin film) ν_{max} 3443, 2960, 2928, 1725, 1366, 1137 cm^{-1}; ^1H NMR ($CDCl_3$, 400 MHz) δ 5.89 (d, J = 7.6 Hz, 1H), 5.87–5.82 (m, 1H), 5.42 (ddd, J = 9.6, 2.4, 2.4 Hz, 1H), 3.00 (dd, J = 2.0, 2.0 Hz, 1H), 2.79–2.72 (m, 2H), 2.64–2.62 (m, 1H), 2.52 (s, 1H), 2.22 (doublet of sept, J = 7.2, 0.8 Hz, 1H), 1.93–1.86 (m, 1H), 1.84–1.75 (m, 1H), 1.61 (dddd, J = 12.4, 10.0,

dx.doi.org/10.1021/jo201658y | *J. Org. Chem.* 2011, 76, 8944–8954

4.8, 4.8 Hz, 1H), 1.23 (s, 3H), 1.21−1.16 (m, 1H), 0.94 (d, J = 6.8 Hz, 3H), 0.92 (d, J = 6.8 Hz, 3H); ^{13}C NMR ($CDCl_3$, 100 MHz) δ 213.6, 144.8, 130.2, 128.4, 125.3, 72.9, 56.3, 49.2, 35.5, 32.9, 31.8, 26.3, 25.9, 23.5, 20.8, 20.5; HRMS-ESI (m/z) $[M + H]^+$ calcd for $C_{16}H_{23}O_2$ 247.1698, found 247.1721; $[\alpha]^{22}_D$ = +160.4° (c = 1.17, $CHCl_3$).

(1*R*,2*S*,3*S*,7*R*,8*S*)-3-Hydroxy-3-methyl-6-(propan-2-yl)-tricyclo[6.2.2.0^{2,7}]dodeca-5,9-dien-4-one (13e). Utilizing the same protocol for compound **12e**, product **13e** (22.5 mg, 25%) was isolated as a white solid: R_f = 0.39 (hexanes/EtOAc 5/1); mp 52−53 °C; IR (thin film) ν_{max} 3463, 2963, 2867, 1673, 1376, 1170 cm^{-1}; ^{1}H NMR ($CDCl_3$, 400 MHz) δ 6.04 (dd, J = 3.2, 3.2 Hz, 1H), 5.84 (s, 1H), 5.77 (dd, J = 3.2, 3.2 Hz, 1H), 3.99 (s, 1H), 2.96 (dddd, J = 4.4, 3.2, 2.0, 2.0 Hz, 1H), 2.83 (dd, J = 8.0, 2.8 Hz, 1H), 2.78 (ddd, J = 4.0, 2.0, 2.0 Hz, 1H), 2.44 (sept, J = 6.8 Hz, 1H), 2.26 (dd, J = 8.4, 1.6 Hz, 1H), 1.64−1.59 (m, 1H), 1.52 (dddd, J = 12.4, 9.2, 2.8, 2.8 Hz, 1H), 1.40 (dddd, J = 12.4, 12.4, 3.2, 3.2 Hz, 1H), 1.27−1.20 (m, 1H), 1.19 (s, 3H), 1.08 (d, J = 6.8 Hz, 3H), 1.07 (d, J = 6.8 Hz, 3H); ^{13}C NMR ($CDCl_3$, 100 MHz) δ 202.5, 170.8, 133.8, 132.7, 119.2, 73.9, 47.9, 45.7, 35.4, 32.8, 32.0, 29.9, 26.1, 24.5, 23.2, 20.9; HRMS-ESI (m/z) $[M + H]^+$ calcd for $C_{16}H_{23}O_2$ 247.1698, found 247.1707; $[\alpha]^{22}_D$ = −128.1° (c = 0.52, $CHCl_3$).

1-[(1*R*,2*S*,3*S*,6*R*,7*S*)-3-Hydroxy-5-(propan-2-yl)tricyclo-[5.2.2.0^{2,6}]undeca-4,8-dien-3-yl]ethanone (14). Utilizing the same protocol for compound **12g**, product **14** (8.2 mg, 9%) was isolated as a white solid: R_f = 0.46 (hexanes/EtOAc 5/1); mp 98−100 °C; IR (thin film) ν_{max} 3450, 2952, 2936, 2915, 1698, 1367, 1102 cm^{-1}; ^{1}H NMR ($CDCl_3$, 500 MHz) δ 6.27 (dd, J = 7.2, 7.2 Hz, 1H), 5.89 (dd, J = 7.2, 7.2 Hz, 1H), 5.03 (dd, J = 1.5, 1.5 Hz, 1H), 3.92 (s, 1H), 2.98 (ddd, J = 8.5, 2.2, 2.2 Hz, 1H), 2.77−2.75 (m, 1H), 2.58−2.55 (dd, J = 2.0 Hz, 1H), 2.34 (dd, J = 8.2, 2.2 Hz, 1H), 2.29 (sept, J = 7.0 Hz, 1H), 2.09 (2, 3H), 1.49 (dddd, J = 12.0, 9.5, 4.5, 2.2 Hz, 1H), 1.41 (dddd, J = 12.0, 9.0, 3.0, 3.0 Hz, 1H), 1.33 (dddd, J = 11.5, 11.5, 3.5, 3.5 Hz, 1H), 1.26−1.20 (m, 1H), 1.06 (d, J = 7.0 Hz, 3H), 1.04 (d, J = 7.0 Hz, 3H); ^{13}C NMR ($CDCl_3$, 100 MHz) δ 210.5, 159.5, 134.0, 129.2, 124.8, 90.8, 53.5, 48.7, 32.7, 30.9, 27.7, 25.1, 24.2, 23.6, 21.7, 20.8; HRMS-ESI (m/z) $[M - H_2O + H]^+$ calcd for $C_{16}H_{21}O$ 229.1592, found 229.1597; $[\alpha]^{22}_D$ = +210.4° (c = 0.30, $CHCl_3$).

Gradifloracin (16). Oxidation of salicyl alcohol benzoate (50.0 mg, 0.17 mmol) according to the reported procedure[12] (1.2 equiv of DIEA, 1.5 equiv of $[(-)$-sparteine$]_2Cu_2O_2(PF_6)_2$, 3 Å MS, O_2, CH_2Cl_2, −78 °C, 40 h) generated dimer **16** as a gray solid (15.0 mg, 28%, 61% brsm) after silica gel chromatography. The ^{1}H, ^{13}C NMR, IR, and HRMS data for **16** were identical with those reported in the literature:[24,25] $[\alpha]^{22}_D$ = −5.1° (c = 0.57, $CHCl_3$; lit. $[\alpha]^{22}_D$ = −13.6°, c = 0.728, $CHCl_3$). The ee for **16** (24%) was determined on the basis of chiral HPLC analysis of its derivative **21**.

Dimer (±)-17. Oxidation of 2,6-dimethylphenol (20.0 mg, 0.164 mmol) according to the reported procedure[12] (1.0 equiv of $LiOH·H_2O$, 1.2 equiv of (N,N'-di-*tert*-butylethylenediamine)$_2Cu_2O_2(PF_6)_2$, 3 Å MS, O_2, CH_2Cl_2, −78 °C, 16 h) generated dimer **17** as a light yellow solid (16.2 mg, 72%) after silica gel chromatography. ^{1}H, ^{13}C NMR, IR, and HRMS data for **17** were identical with those reported in the literature.[25]

(1*R*,2*S*,6*R*,7*S*,9*R*)-11-*tert*-Butyl-9-hydroxy-9-methyltricyclo-[5.2.2.0^{2,6}]undeca-4,10-dien-8-one (19). Dimer (+)-**15** (30.0 mg, 0.083 mmol) and dicyclopentadiene (**18**; 54.9 mg, 0.415 mmol) were thermolyzed according to the general procedure. The crude mixture was purified by silica gel chromatography (hexanes/EtOAc 15/1) to afford product **19** (38.0 mg, 93%) as a white solid: R_f = 0.26 (hexanes/EtOAc 7/1); mp 92−93 °C; IR (thin film) ν_{max} 3425, 2963, 2928, 1721, 1364 cm^{-1}; ^{1}H NMR ($CDCl_3$, 400 MHz) δ 5.85 (dd, J = 6.8, 2.0 Hz, 1H), 5.62−5.59 (m, 1H), 5.34−5.32 (m, 1H), 3.25 (dd, J = 2.0, 2.0 Hz, 1H), 3.20−3.10 (m, 2H), 2.83 (dddd, J = 9.2, 4.8, 2.4, 2.4 Hz, 1H), 2.63 (bs, 1H), 2.46 (ddddd, J = 16.8, 9.2, 2.0, 2.0, 2.0 Hz, 1H), 1.94 (ddddd, J = 16.8, 6.0, 2.0, 2.0, 2.0 Hz, 1H), 1.21 (s, 3H), 0.92 (s, 9H); ^{13}C NMR ($CDCl_3$, 100 MHz) δ 214.9, 148.7, 132.8, 130.4, 122.2, 73.2, 52.6, 50.0, 47.5, 38.2, 34.2, 33.2, 28.2 (three carbons overlapping), 26.3; HRMS-ESI (m/z) $[M - H_2O + H]^+$ calcd for $C_{16}H_{21}O$ 229.1592, found 229.1604; $[\alpha]^{22}_D$ = −90.0° (c = 0.65, $CHCl_3$).

(1*R*,2*S*,6*R*,7*S*,9*S*)-11-*tert*-Butyl-9-hydroxy-9-methyl-3,5-dioxatricyclo[5.2.2.0^{2,6}]undec-10-ene-4,8-dione (20). Dimer (+)-**15** (30.0 mg, 0.083 mmol) and methyl vinyl ketone (**9**; 105.4 μL, 1.66 mmol) were thermolyzed by following the general procedure. The crude mixture was purified by silica gel chromatography (hexanes/EtOAc 5/1 to 3/1) to afford product **20** (34.8 mg, 78%) as a colorless oil: R_f = 0.13 (hexanes/EtOAc 3/1); IR (thin film) ν_{max} 3423, 2965, 1786, 1731, 1367, 1162, 1058 cm^{-1}; ^{1}H NMR ($CDCl_3$, 400 MHz) δ 5.99 (d, J = 6.8, 1.2 Hz, 1H), 5.36 (dd, J = 8.0, 3.6 Hz, 1H), 5.03 (dd, J = 8.0, 3.2 Hz, 1H), 3.81 (dd, J = 3.6, 2.0 Hz, 1H), 3.39 (dd, J = 6.8, 3.2 Hz, 1H), 2.56 (bs, 1H), 1.31 (s, 3H), 1.04 (s, 9H); ^{13}C NMR ($CDCl_3$, 100 MHz) δ 205.8, 154.4, 147.9, 121.2, 74.5, 74.2, 71.8, 52.9, 45.6, 34.9, 27.8 (three carbons overlapping), 25.3; HRMS-ESI (m/z) $[2M + H]^+$ calcd for $C_{28}H_{37}O_{10}$ 533.2387, found 533.2399; $[\alpha]^{22}_D$ = −176.9° (c = 1.09, $CHCl_3$).

(12-Hydroxy-13-oxotetracyclo[9.2.2.0^{2,10}.0^{3,8}]pentadeca-3,5,7,14-tetraen-12-yl)methyl Benzoate (21). Gradifloracin (**16**; 10.0 mg, 0.020 mmol) and indene (**9b**; 23.3 μL, 0.20 mmol) in mesitylene were irradiated in a microwave reactor at 170 °C for 15 min. Following the general procedure, the obtained crude mixture was purified by silica gel chromatography (hexanes/EtOAc 10/1 to 8/1) to afford product **21** (11.8 mg, 80%) as a light yellow oil: R_f = 0.38 (hexanes/EtOAc 3/1). IR (thin film) ν_{max} 3443, 2917, 2849, 1726, 1692, 1272 cm^{-1}; ^{1}H NMR ($CDCl_3$, 400 MHz) δ 8.08 (dd, J = 8.4, 1.2 Hz, 2H), 7.60−7.56 (m, 1H), 7.45 (dd, J = 8.4, 8.4 Hz, 2H), 7.19−7.13 (m, 3H), 7.12−7.09 (m, 1H), 6.35 (dd, J = 7.2, 7.2 Hz, 1H), 5.94 (dd, J = 7.2, 7.2 Hz, 1H), 4.45 (d, J = 12.0 Hz, 1H), 4.28 (d, J = 12.0 Hz, 1H), 3.83 (dd, J = 9.2, 2.0 Hz, 1H), 3.57 (ddd, J = 6.4, 2.8, 1.2 Hz, 1H), 3.50−3.43 (m, 1H), 3.29 (ddd, J = 6.4, 2.8, 1.2 Hz, 1H), 3.23 (dd, J = 16.8, 10.4 Hz, 1H), 3.13 (s, 1H), 2.69 (dd, J = 16.8, 4.4 Hz, 1H); ^{13}C NMR ($CDCl_3$, 100 MHz) δ 209.9, 166.6, 144.3, 142.4, 133.3, 133.2, 129.8 (two carbons overlapping), 129.6, 128.6, 128.5 (two carbons overlapping), 127.3, 126.7, 124.4, 124.0, 74.3, 68.4, 53.1, 50.1, 45.4, 37.7, 33.9; HRMS-ESI (m/z) $[M + Na]^+$ calcd for $C_{23}H_{20}NaO_4$ 383.1259, found 383.1252; $[\alpha]^{22}_D$ = −22.3° (c = 0.24, $CHCl_3$). The ee for **21** (24%) was determined by using a Waters Breeze HPLC System (ChiralPak AD-H, 150 × 4.6 mm, 10% isopropyl alcohol in hexane, 1.0 mL/min, retention time 12.3 min (minor enantiomer) and 14.6 min (major enantiomer)) using UV detection at 254 nm.

9-Hydroxy-7,9-dimethyl-4-phenyl-4-azatricyclo[5.2.2.0^{2,6}]-undec-10-ene-3,5,8-trione (22). Dimer **17** (20.0 mg, 0.072 mmol) and *N*-phenylmaleimide (**6**; 37.4 mg, 0.216 mmol) were thermolyzed by following the general procedure. The crude mixture was purified by silica gel chromatography (hexanes/EtOAc 2/1) to afford product **2** (44.6 mg, 99%) as a light yellow solid: R_f = 0.08 (hexanes/EtOAc 3/1); mp 161−163 °C; IR (thin film) ν_{max} 3444, 2977, 1703, 1698, 1385, 1186 cm^{-1}; ^{1}H NMR ($CDCl_3$, 400 MHz) δ 7.45−7.40 (m, 2H), 7.39−7.34 (m, 1H), 7.17 (dd, J = 7.6, 1.6 Hz, 2H), 6.42 (dd, J = 8.4, 6.4 Hz, 1H), 5.95 (dd, J = 8.4, 1.2 Hz, 1H), 3.85 (dd, J = 8.4, 3.6 Hz, 1H), 3.54 (ddd, J = 6.4, 3.2, 1.6 Hz, 1H), 2.96 (d, J = 8.0 Hz, 1H), 2.95 (s, 1H), 1.57 (s, 3H), 1.32 (s, 3H); ^{13}C NMR ($CDCl_3$, 100 MHz) δ 210.3, 177.1, 174.4, 133.9, 132.9, 131.6, 129.1 (two carbons overlapping), 128.7, 126.4 (two carbons overlapping), 70.8, 50.5, 45.4, 44.9, 40.9, 25.6, 14.8; HRMS-ESI (m/z) $[M + H]^+$ calcd for $C_{18}H_{18}NO_4$ 312.1236, found 312.1249.

12-Hydroxy-12-methyl-14-(propan-2-yl)tetracyclo-[9.2.2.0^{2,10}.0^{3,8}]pentadeca-3,5,7,14-tetraen-13-one (23). Dimer **17** (20.0 mg, 0.072 mmol) and indene (**11**; 83.9 μL, 0.72 mmol) were thermolyzed by following the general procedure. The crude mixture was purified by preparative TLC (hexanes/EtOAc 3/1) to afford product **23** (28.7 mg, 78%) as a light yellow solid. The ^{1}H, ^{13}C NMR, IR, and HRMS dataf or **16** were identical with those reported in the literature.[1a]

8-Hydroxy-1,8-dimethyl-3-oxatricyclo[5.2.2.0^{2,6}]undec-10-en-9-one (24). Dimer **17** (20.0 mg, 0.072 mmol) and 2,3-dihydrofuran **9d** (111.9 μL, 1.48 mmol) were thermolyzed following the general procedure. The concentrated mixture was dissolved in 2

mL of CH_2Cl_2 followed by addition of MP-TsOH resin (100 mg), and the reaction mixture was shaken for 30 min. The MP-TsOH resin was filtered away, and the filtrate was concentrated. The crude mixture was purified by silica gel chromatography (hexanes/EtOAc 8/1 to 7/1) to afford product **24** (25.6 mg, 85%) as a white solid: R_f = 0.27 (hexanes/EtOAc 2/1); mp 117−119 °C; IR (thin film) ν_{max} 3429, 2973, 2933, 1726, 1451, 1366, 1080 cm^{-1}; ^1H NMR ($CDCl_3$, 400 MHz) δ 6.33 (dd, J = 7.2, 7.2 Hz, 1H), 5.75 (dd, J = 8.4, 1.6 Hz, 1H), 3.89−3.82 (m, 2H), 3.53 (ddd, J = 8.4, 8.4, 8.4 Hz, 1H), 3.18 (ddd, J = 8.4, 8.4, 8.4 Hz, 1H), 2.92−2.90 (m, 1H), 2.50 (s, 1H), 2.10−2.00 (m, 1H), 1.64−1.55 (m, 1H), 1.32 (s, 3H), 1.24 (s, 3H); ^{13}C NMR ($CDCl_3$, 100 MHz) δ 213.4, 134.1, 132.6, 84.5, 71.9, 69.1, 55.1, 46.4, 39.0, 30.9, 26.5, 14.5; LRMS m/z (% relative intensity): 231.1 [$(M + Na)^+$, 31], 191.1 (100), 163.1 (70), 141.1 (34) .

9-Hydroxy-11-methyl-4-phenyl-9-(propan-2-yl)-4-azatricyclo[5.2.2.0^{2,6}]undec-10-ene-3,5,8-trione (25). Dimer **18** (30.0 mg, 0.090 mmol) and *N*-phenylmaleimide (**6**; 46.9 mg, 0.271 mmol) in mesitylene were thermolyzed by following the general procedure. The crude mixture was purified by silica gel chromatography (hexanes/EtOAc 6/1 to 5/1) to afford product **25** (49.1 mg, 80%) as a white solid: R_f = 0.31 (hexanes/EtOAc 2/1); mp 169−170 °C; IR (thin film) ν_{max} 3480, 2966, 2924, 1708, 1500, 1383, 1187 cm^{-1}; ^1H NMR ($CDCl_3$, 400 MHz) δ 7.45−7.41 (m, 2H), 7.38−7.35 (m, 1H), 7.14 (dd, J = 7.2, 1.2 Hz, 2H), 6.03 (ddd, J = 6.4, 1.6, 1.6 Hz, 1H), 3.68 (dd, J = 8.0, 3.2 Hz, 1H), 3.59 (dd, J = 3.2, 1.6 Hz, 1H), 3.56 (dd, J = 6.4, 3.2 Hz, 1H), 3.36 (dd, J = 8.0, 3.2 Hz, 1H), 2.46 (s, 1H), 1.87 (sept, J = 6.8 Hz, 1H), 1.84 (d, J = 1.6 Hz, 3H), 0.98 (d, J = 6.8 Hz, 3H), 0.82 (d, J = 6.8 Hz, 3H); ^{13}C NMR ($CDCl_3$, 100 MHz) δ 209.4, 177.5, 175.1, 136.0, 131.6, 129.1(two carbons overlapping), 128.8, 126.3 (two carbons overlapping), 125.0, 75.9, 53.5, 42.9, 42.2, 39.8, 33.2, 20.7, 17.8, 16.2; HRMS-ESI (m/z) $[M + H]^+$ calcd for $C_{20}H_{22}NO_4$ 340.1549, found 340.1553.

Computational Methods. All calculations were carried out with Gaussian 03 revision E.01,[39] Spartan 06, or Spartan 08.[40] Structures were optimized and characterized by frequency analysis at the B3LYP/6-31G(d) level of theory with all transition states showing a single imaginary vibrational mode corresponding to the expected reaction.[41] Unscaled zero point vibrational energy (ZPVE) corrections have been applied to total energies. Energies and geometries for stationary points are summarized in the Supporting Information. Solvation was not included in these calculations, because it is expected that our nonpolar solvents would not significantly affect reaction energetics.

■ ASSOCIATED CONTENT

Ⓢ Supporting Information

Text, figures, and a CIF file giving experimental procedures and characterization data for all new compounds, including X-ray structure analysis of compound **10e**, X-ray crystallographic data, and detailed computational methods and results. This material is available free of charge via the Internet at http://pubs.acs.org.

■ AUTHOR INFORMATION

Corresponding Author

*E-mail: porco@bu.edu; richard.johnson@unh.edu.

■ ACKNOWLEDGMENTS

This work was generously supported by the NIGMS CMLD Initiative (P50 GM067041, J.A.P.), the National Science Foundation (CHE-0910826, R.P.J.), and the Intramural Research Program of the NIH, National Cancer Institute, Center for Cancer Research. This project has been funded in part with federal funds from the National Cancer Institute, National Institutes of Health, under contract HHSN261200800001E. The content of this publication does not necessarily reflect the views or policies of the Department of Health and Human Services, nor does mention of trade names, commercial products or organizations imply endorsement by the U.S. Government. We thank Dr. Emil Lobkovsky (Cornell University) for X-ray crystal structure analysis and Anton Paar Corp., CEM Corp., and Waters Corp. for assistance with instrumentation.

■ REFERENCES

(1) For use of *o*-quinol dimers in retro-[4 + 2]/[4 + 2] cascades, see: (a) Singh, V. K.; Deota, P. T.; Bedekar, A. V. *J. Chem. Soc., Perkin Trans. 1* **1992**, 903. (b) Singh, V.; Samanta, B. *Tetrahedron Lett.* **1999**, *40*, 1807.

(2) Dong, S.; Hamel, E.; Bai, R.; Covell, D. G.; Beutler, J. A.; Porco, J. A. Jr. *Angew. Chem.; Int. Ed.* **2009**, *48*, 1494.

(3) For use of MOB-derived dimers, see: (a) Liao, C. C.; Peddinti, R. K. *Acc. Chem. Res.* **2002**, *35*, 856. (b) Chittimalla, S. K.; Shiao, H. Y.; Liao, C. C. *Org. Biomol. Chem.* **2006**, *4*, 2267. (c) Snyder, S. A.; Kontes, F. *J. Am. Chem. Soc.* **2009**, *131*, 1745.

(4) For reviews on *o*-quinol and MOB-derived [4 + 2] cyclodimers, see: (a) Magdziak, D.; Meek, S. J.; Pettus, T. R. R. *Chem. Rev.* **2004**, *104*, 1383. (b) Quideau, S.; Pouysegu, L.; Deffieux, D. *Synlett* **2008**, 467.

(5) Kappe, C. O. *Chem. Soc. Rev.* **2008**, *37*, 1127.

(6) For a recent review on use of graphite in microwave reactions, see: (a) Besson, T.; Thiery, V.; Dubac, J. *Microwaves in Organic Synthesis*, 2nd ed.; Wiley-VCH: Weinheim, Germany, 2006; Vol. *1*, p 416. For a recent example employing graphite, see: (b) Cho, H. Y.; Ajaz, A.; Himali, D.; Waske, P. A.; Johnson, R. P. *J. Org. Chem.* **2009**, *74*, 4137.

(7) (a) Kremsner, J. M.; Kappe, C. O. *J. Org. Chem.* **2006**, *71*, 4651. (b) Razzaq, T.; Kremsner, J. M.; Kappe, C. O. *J. Org. Chem.* **2008**, *73*, 6321. For silicon carbide, see: (c) *Properties of Silicon Carbide*; Harris, G. L., Ed.; Institute of Electrical Engineers: London, 1995. (d) *Silicon Carbide: Recent Major Advances*; Choyke, W. J., Matsunami, H., Pensl, G., Eds.; Springer: Berlin, 2004. (e) *Advances in Silicon Carbide Processing and Applications*; Saddow, S. E., Agarwal, A, Eds.; Artech House: Norwood, MA, 2004.

(8) Damm, M.; Kappe, C. O. *Mol. Diversity* **2009**, *13*, 529.

(9) Kremsner, J. M.; Stadler, A; Kappe, C. O. *J. Comb. Chem.* **2007**, *9*, 285. (b) Damm, M.; Kappe, C. O. *J. Comb. Chem.* **2009**, *11*, 460.

(10) Beeler, A. B.; Su, S.; Singleton, C. A.; Porco, J. A. Jr. *J. Am. Chem. Soc.* **2007**, *129*, 1413.

(11) (a) Li, C.; Johnson, R. P.; Porco, J. A. Jr. *J. Am. Chem. Soc.* **2003**, *125*, 5095−5106. (b) Lei, X.; Johnson, R. P.; Porco, J. A. Jr. *Angew. Chem., Int. Ed.* **2003**, *42*, 3913.

(12) Dong, S.; Zhu, J.; Porco, J. A. Jr. *J. Am. Chem. Soc.* **2008**, *130*, 2738.

(13) See the Supporting Information for complete instrumentation and experimental details.

(14) For UPLC, see: (a) Mazzeo, J. R.; Neue, U. D.; Kele, M.; Plumb, R. S. *Anal. Chem.* **2005**, *77*, 460A. (b) Nováková, L.; Matysová, L.; Solich, P. *Talanta* **2006**, *68*, 908.

(15) For a recent review on the dienone−phenol rearrangement, see: Whiting, D. A. In *Comprehensive Organic Syntheses*; Trost, B. M., Fleming, I., Eds.; Pergamon Press: Oxford, U.K., 1991; Vol. *3*, pp 803−821.

(16) Carman, R. M.; Van Dongen, J. M. A. M. *Aust. J. Chem.* **1984**, *37*, 2607.

(17) Wannere, C. S.; Paul, A.; Herges, R.; Houk, K. N.; Schaefer, H. F. III; Schleyer, P. v. R. *J. Comput. Chem.* **2007**, *28*, 344.

(18) Snider, B. B.; Chen, Z. *Org. Prep. Proced. Int.* **1999**, *31*, 537.

(19) Kuo, Y. H.; Chen, C. H.; Huang, S. L. *Chem. Pharm. Bull.* **1999**, *46*, 181.

(20) Competition between Cope rearrangements and retro-Diels−Alder reactions in similar bicyclic structures has been reported: (a) Su, K.-J.; Mieusset, J.-L.; Arion, V. B.; Brecker, L.; Brinker, U. H. *Org. Lett.* **2007**, *9*, 113. (b) Jeong, J.-P.; Lee, O.-S.; Yang, K. *Bull. Korean Chem. Soc.* **2002**, *23*, 829. (c) Singh, V.; Sharma, U.; Prasanna, V.; Porinchu, M. *Tetrahedron* **1995**, *51*, 6015.

(21) For [3,3]-sigmatropic rearrangement of bridged 1,5-dienes, see: Bultman, M. S.; Ma, J.; Gin, D. Y. *Angew. Chem., Int. Ed.* **2008**, *47*, 6821 and references cited therein.
(22) Paquette, L. A.; Hofferberth, J. E. *Org. React.* **2003**, *62*, 477.
(23) (a) Nagahama, S.; Tazaki, M. *Bull. Chem. Soc. Jpn.* **1987**, *60*, 4175. (b) Shimizu, T.; Hiranuma, S.; Qian, Z.-H.; Yoshioka, H. *Synlett* **1991**, 725.
(24) Liao, Y. H.; Xu, L. Z.; Yang, S. L.; Dai, J.; Zhen, Y. S.; Zhu, M.; Sun, N. J. *Phytochemistry* **1997**, *45*, 729.
(25) Gagnepain, J.; Castet, F.; Quideau, S. *Angew. Chem., Int. Ed.* **2007**, *46*, 1533.
(26) Dory, Y. L.; Roy, A.-L.; Soucy, P.; Deslongchamps, P. *Org. Lett.* **2009**, *11*, 1197.
(27) Gagnepain, J.; Mereau, R.; Dejugnac, D.; Leger, J.-M.; Castet, F.; Deffieux, D.; Pouysegu, L.; Quideau, S. *Tetrahedron* **2007**, *63*, 6493.
(28) Details of computational methods and results are presented in the Supporting Information.
(29) (a) Cieplak, A. S. *J. Am. Chem. Soc.* **1981**, *103*, 4540. (b) Macaulay, J. B.; Fallis, A. G. *J. Am. Chem. Soc.* **1990**, *112*, 1136.
(30) Hou, H.-F.; Peddinti, R. K.; Liao, C.-C. *Org. Lett.* **2002**, *4*, 2477.
(31) In each case, we find that the transition state DFT wavefunction is stable relative to becoming an open shell. Thus, these reactions may be described as asynchronous but concerted. Further examples of transition-state structures are shown in the Supporting Information.
(32) Miller, B. *Acc. Chem. Res.* **1975**, *8*, 245 and references therein.
(33) Ruocco, K. M.; Goncharova, E. I.; Young, M. R.; Colburn, N. H.; McMahon, J. B.; Henrich, C. J. *J. Biomol. Screen.* **2007**, *12*, 133.
(34) Booth, N. L.; Sayers, T. J.; Brooks, A. D.; Thomas, C. F.; Jacobsen, K.; Goncharova, E. I.; McMahon, J. B.; Henrich, C. J. *Cancer Immunol. Immunother.* **2009**, *58*, 1229.
(35) Woldemichael, G. M.; Vasselli, J. R.; Gardella, R. S.; McKee, T. C.; Linehan, W. M.; McMahon, J. B. *J. Biomol. Screen.* **2006**, *11*, 678.
(36) Young, M. R.; Li, J.; Rincon, M.; Flavell, R. A.; Sathyanarayana, B. K.; Hunziker, R. *Proc. Natl. Acad. Sci. U.S.A.* **1999**, *96*, 9827.
(37) Rodriguez, A. M.; Prieto, P.; de la Hoz, A.; Díaz-Ortiz, A. *Org. Biomol. Chem.* **2011**, *9*, 2371.
(38) Lebel, H.; Paquet, V. *J. Am. Chem. Soc.* **2004**, *126*, 320.
(39) Frisch, M. J.; Trucks, G. W.; Schlegel, H. B.; Scuseria, G. E.; Robb, M. A.; Cheeseman, J. R.; Montgomery, Jr., J. A.; Vreven, T.; Kudin, K. N.; Burant, J. C.; Millam, J. M.; Iyengar, S. S.; Tomasi, J.; Barone, V.; Mennucci, B.; Cossi, M.; Scalmani, G.; Rega, N.; Petersson, G. A.; Nakatsuji, H.; Hada, M.; Ehara, M.; Toyota, K.; Fukuda, R.; Hasegawa, J.; Ishida, M.; Nakajima, T.; Honda, Y.; Kitao, O.; Nakai, H.; Klene, M.; Li, X.; Knox, J. E.; Hratchian, H. P.; Cross, J. B.; Bakken, V.; Adamo, C.; Jaramillo, J.; Gomperts, R.; Stratmann, R. E.; Yazyev, O.; Austin, A. J.; Cammi, R.; Pomelli, C.; Ochterski, J. W.; Ayala, P. Y.; Morokuma, K.; Voth, G. A.; Salvador, P.; Dannenberg, J. J.; Zakrzewski, V. G.; Dapprich, S.; Daniels, A. D.; Strain, M. C.; Farkas, O.; Malick, D. K.; Rabuck, A. D.; Raghavachari, K.; Foresman, J. B.; Ortiz, J. V.; Cui, Q.; Baboul, A. G.; Clifford, S.; Cioslowski, J.; Stefanov, B. B.; Liu, G.; Liashenko, A.; Piskorz, P.; Komaromi, I.; Martin, R. L.; Fox, D. J.; Keith, T.; Al-Laham, M. A.; Peng, C. Y.; Nanayakkara, A.; Challacombe, M.; Gill, P. M. W.; Johnson, B.; Chen, W.; Wong, M. W.; Gonzalez, C.; and Pople, J. A. *Gaussian 03, Revision E.01*; Gaussian Inc., Wallingford, CT, 2004.
(40) *Spartan 06 and Spartan 08*; Wavefunction Inc., Irvine, CA.
(41) (a) Kohn, W.; Becke, A. D.; Parr, R. G. *J. Phys. Chem.* **1996**, *100*, 12974. (b) Becke, A. D. *J. Chem. Phys.* **1993**, *98*, 5648. (c) Lee, C.; Yang, Y.; Parr, R. G. *Phys. Rev. B* **1988**, *37*, 785.